Relative Biological Effectiveness and Non-Poissonian Distribution of Dicentric Chromosome Aberrations following Californium-252 Neutron Exposures of Human Peripheral Blood Lymphocytes

Authors: Paterson, Laura C., Yonkeu, Andre, Ali, Fawaz, Priest, Nicholas D., Boreham, Douglas R., et al.

Source: Radiation Research, 195(2) : 211-217

Published By: Radiation Research Society

URL: https://doi.org/10.1667/RR15528.2

RADIATION RESEARCH **195**, 211–217 (2021)
0033-7587/21 $15.00

DOI: 10.1667/RR15528.2

SHORT COMMUNICATION

Relative Biological Effectiveness and Non-Poissonian Distribution of Dicentric Chromosome Aberrations following Californium-252 Neutron Exposures of Human Peripheral Blood Lymphocytes

Laura C. Paterson,[a,b] Andre Yonkeu,[a] Fawaz Ali,[a] Nicholas D. Priest,[a,1] Douglas R. Boreham,[c,d] Colin B. Seymour,[c] Farrah Norton[a] and Richard B. Richardson[a,b,2]

[a] *Canadian Nuclear Laboratories, Chalk River, Canada;* [b] *McGill University, Montreal, Canada;* [c] *McMaster University, Hamilton, Canada; and* [d] *Northern Ontario School of Medicine, Sudbury, Canada*

Paterson, L. C., Yonkeu, A., Ali, F., Priest, N. D., Boreham, D. R., Seymour, C. B., Norton, F., Richardson, R. B. Relative Biological Effectiveness and Non-Poissonian Distribution of Dicentric Chromosome Aberrations following Californium-252 Neutron Exposures of Human Peripheral Blood Lymphocytes. *Radiat. Res*. 195, 211–217 (2021).

Cells exposed to fast neutrons often exhibit a non-Poisson distribution of chromosome aberrations due to the high ionization density of the secondary reaction products. However, it is unknown whether lymphocytes exposed to californium-252 (^{252}Cf) spectrum neutrons, of mean energy 2.1 MeV, demonstrate this same dispersion effect at low doses. Furthermore, there is no consensus regarding the relative biological effectiveness (RBE) of ^{252}Cf neutrons. Dicentric and ring chromosome formations were assessed in human peripheral blood lymphocytes irradiated at doses of 12–135 mGy. The number of aberrations observed were tested for adherence to a Poisson distribution and the maximum low-dose relative biological effectiveness (RBE_M) was also assessed. When ^{252}Cf-irradiated lymphocytes were examined along with previously published cesium-137 (^{137}Cs) data, RBE_M values of 15.0 ± 2.2 and 25.7 ± 3.8 were found for the neutron-plus-photon and neutron-only dose components, respectively. Four of the five dose points were found to exhibit the expected, or close to the expected non-Poisson over-dispersion of aberrations. Thus, even at low doses of ^{252}Cf fast neutrons, when sufficient lymphocyte nuclei are scored, chromosome aberration clustering can be observed.

INTRODUCTION

Californium-252 has a mean neutron energy of 2.1 MeV (*1*) and is routinely utilized in the petroleum industry and in nuclear power production (*2*). As such, understanding the biological effects and hazards of low-dose ^{252}Cf neutron exposures is important for worker protection. Neutrons are very useful for examining biological mechanisms dependent on ionizing density or linear energy transfer (LET) due to the wide range of energies that result in variable relative biological effectiveness (RBE). Our group is currently engaged in quantifying a suite of cellular end points at multiple neutron energies, including thermal neutrons (*3*) and, in the current work, fast neutrons.

Dicentric and ring chromosome analysis in human peripheral blood lymphocytes is currently considered the gold-standard biological dosimetry method, with studies establishing direct correlations between dicentric and (much rarer) ring chromosome induction and absorbed dose after low- and high-LET irradiations (*4*).

RBE indicates the ability of a particular radiation type to produce a certain biological effect, as compared to a reference radiation, typically low-LET gamma or X rays. RBE is an experimentally determined unit-less quantity that influences radiation weighting factors (denoted by w_R), theoretically determined values put forth by the International Commission on Radiological Protection (ICRP) to account for the varying biological effects induced by different radiations. However, unlike w_R, which takes into account all possible biological consequences of a particular radiation, RBE values vary with dose, dose rate, biological end point and cell type (*5*) and consequently will not necessarily equal the w_R values. The RBE for dicentric and ring chromosome induction in peripheral blood lymphocytes after neutron exposure has previously been examined at many different incident energies and is reported to peak around 0.385 MeV (RBE_M of 94.4 ± 38.9) (*6*). In two published studies, RBE was evaluated for human peripheral

Editor's note. The online version of this article (DOI: https://doi.org/10.1667/RR15528.2) contains supplementary information that is available to all authorized users.

[1] Retired.

[2] Address for correspondence: Chalk River Laboratories, Canadian Nuclear Laboratories, 286 Plant Road, Station 51A, Chalk River, ON K0J 1J0, Canada; email: richard.richardson@cnl.ca.

TABLE 1
Comparison of ^{252}Cf Neutron Studies Examining Dicentric Chromosome Induction in Human Peripheral Blood Lymphocytes

Literature	No.	Dose range (mGy)	Dose rate (mGy h^{-1})	Reference radiation	No. of cells analyzed per dose point	$\alpha \pm$ SE (Gy^{-1})	RBE $\pm$ SE or [RBE$_M$ $\pm$ SE]
(*7*)	1.	180 – 4,428 [n + γ]	120 and 170	^{60}Co	100 – 540 (μ = 236)	0.0043 $\pm$ 0.0010	[24 $\pm$ 11[a]]
	2.	118 – 2,894 [n]	120 and 170	^{60}Co	100 – 540 (μ = 236)	0.006 $\pm$ 0.00019	6–27[b] [33 $\pm$ 15[a]]
(*8*)	1.	50 – 2,500 [n + γ]	1,200	^{60}Co	200 – 1,103 (μ = 598)	0.369	2.3[c] [6.3[a]]
	2.	30 – 1,620 [n]	1,200	^{60}Co	200 – 1,103 (μ = 598)	0.581	3.3[c] [9.8[a]]
	3.	500 – 3,000 [n + γ]	120	^{137}Cs	93 – 596 (μ = 325)	0.3	7.6[c] [6.9[a]]
	4.	320 – 1,940 [n]	120	^{137}Cs	93 – 596 (μ = 325)	0.464	11.0[c] [10.6[a]]
	5.	250 – 850 [n + γ]	12	^{137}Cs	600 – 883 (μ = 671)	0.364	7.7[c] [7.7[a]]
	6.	160 – 550 [n]	12	^{137}Cs	600 – 883 (μ = 671)	0.561	12.0[c] [11.9[a]]
Current study	1.	12 – 135 [n + γ]	18.58	^{137}Cs	1,000	1.0490 $\pm$ 0.0747[d]	8–13[e] [15.0 $\pm$ 2.2]
	2.	7 – 75 [n]	10.49	^{137}Cs	1,000	1.7990 $\pm$ 0.1355[d]	13–23[e] [25.7 $\pm$ 3.8]

[a] Calculated in the present study using previously reported data.
[b] Range reflects RBE values calculated at each dose point.
[c] Calculated at 1,000 mGy in the original study.
[d] Regression data is presented in Table 3.
[e] Dose-specific RBE values presented in Table 2.
Note. α = alpha equation coefficient; n = neutron dose component; n + γ = neutron and photon dose components; RBE = relative biological effectiveness; RBE$_M$ = maximum low-dose relative biological effectiveness; SE = standard error; μ: population mean.

blood lymphocytes after ^{252}Cf exposures, as outlined in Table 1. Lloyd *et al*. reported values between 6 and 27 for neutron-only exposures, depending on the dose at which RBE was calculated (*7*). Tanaka *et al*. noted dose-specific RBE values from 2.3 to 7.7 (for neutron and gamma components of ^{252}Cf exposure) and 3.3 to 12.0 (for only the neutron component of the exposure), depending on dose rate (*8*). To compare, ICRP Publication 103 indicates that the w_R of ^{252}Cf is 16.85 (*9*). This value was obtained using the coarse ^{252}Cf neutron energy spectrum (*10*) and the piecewise mathematical equation for w_R stated in (*9*), where the spectrum-averaged w_R value is equal to the sum of the w_R for each energy bin, evaluated at the mid-point energy of the bin, that in turn is weighted by the neutron fluence rate of the bin normalized to the energy-integrated neutron fluence rate.

It is generally accepted that non-Poisson over-dispersion of radiation-induced DNA aberration clustering is a result of either: 1. a partial-body exposure; or 2. a high-LET radiation exposure (*4, 11*), like the ^{252}Cf exposures examined here. In addition to the differing RBE values, neither Lloyd *et al*. (*7*) nor Tanaka *et al*. (*8*) provide a description of the dicentric distribution data necessary to determine whether ^{252}Cf exposures produce the predicted high-LET over-dispersion of the numerical binning of dicentric chromosomes (*4*). Here we present our methods, results and comments for the ^{252}Cf RBE and the associated DNA aberration dispersion.

MATERIALS AND METHODS

Blood was drawn by venipuncture from a healthy male blood donor (aged between 25 and 30 years old) who routinely donates anonymously for other radiobiology work at Canadian Nuclear Laboratories (CNL; Chalk River, Canada) (*12, 13*). Enrollment of a single donor is quite common in prominent neutron studies (*6, 7, 14*), and it is well documented that this individual's blood cells respond normally to low-LET radiation exposures (*12, 13*). After venipuncture, 1.5-ml aliquots of anticoagulated whole blood were transferred into 15-ml polypropylene test tubes with 1-mm-thick walls, and then transferred to the irradiation facility. All samples were maintained at room temperature prior to, and during the irradiations to minimize the effects of concurrent DNA repair (*4*).

^{252}Cf spontaneous fission source irradiations were completed in the Health Physics Neutron Generator facility at CNL. Polypropylene test tubes containing fresh human blood were suspended around the ^{252}Cf source in the middle of the facility. As shown in Fig. 1, blood samples were positioned 10 cm away from the ^{252}Cf pellet (center-to-center distance) and at a height of approximately 103 cm from the facility floor. A REM-500 tissue-equivalent proportional counter, with an internal ^{244}Cm source (*15*), was placed alongside the blood tubes to verify a constant dose rate during blood irradiation.

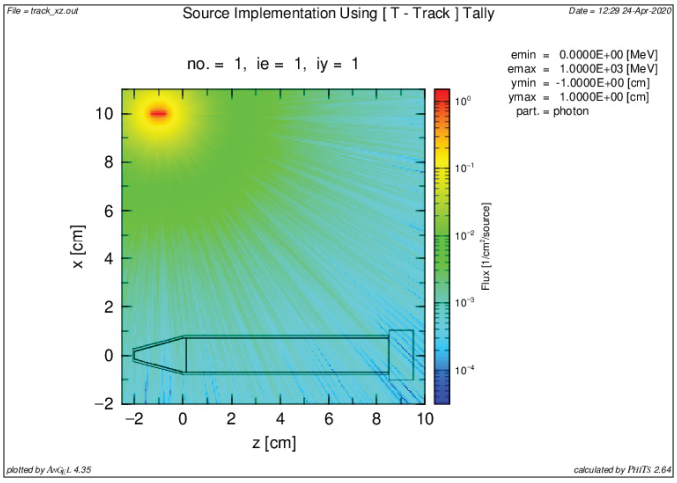

FIG. 1. Contour plot of the spatial intensity of the irradiation environment, showing a side view of the irradiation of the blood volume contained inside the tube holder. The ''hot spot'' shows the location of the radiation source. This image is applicable to both neutron and photon irradiation.

Analytical calculations and Monte Carlo radiation transport simulations were carried out using the Particle and Heavy Ion Transport code System (PHITS) version 2.64 (*16*) to quantify the absorbed dose rate delivered to an individual blood volume contained inside the tube holder by neutrons and photons emitted from ^{252}Cf spontaneous fission, evaluated at the approximate mid-point date of the irradiation campaign. In the PHITS simulations, the T – Deposit tally was used to quantify the total kinetic energy deposited, per source particle, by secondary charged particles in the blood volume and the [T – Track] tally was used to quantify the energy-integrated incident particle fluence, per source particle, through the blood volume.

In the PHITS simulation environment, the blood volume, tube holder and radiation source were surrounded by a sphere of 100-cm radius and filled with air (air also filled the region within the tube holder above the blood volume and below the tube cap). In addition, the simulation utilized the following isotopic composition (by weight fraction) for blood, polypropylene and air (*17*): blood (1.06 g cm^{-3}) consists of ^{1}H (0.101866), ^{nat}C (0.100020), ^{14}N, (0.029640) and ^{16}O (0.759414); polypropylene (0.90 g cm^{-3}) consists of ^{1}H (0.143711) and ^{nat}C (0.856289); and air (0.001205 g cm^{-3}) consists of ^{nat}C (0.000124), ^{14}N (0.755268), ^{16}O (0.231781) and ^{nat}Ar (0.012827). Dose calculations pertaining to ^{252}Cf neutrons utilized the neutron energy spectrum listed in (*18*) and dose calculations pertaining to ^{252}Cf photons utilized the photon energy spectrum and photon emission data listed in (*10*). Using ^{252}Cf neutron emission data described in (*19*) and ^{252}Cf photon emission data described in (*10*), the neutron emission rate at the time of irradiations was $1.29 \times 10^{8} \pm 0.06 \times 10^{8}$ neutrons s^{-1} [the cumulative uncertainty on the neutron emission rate of the source is 5% (*19*)], the direct neutron fluence rate and direct photon fluence rate incident on the blood volume at the time of irradiation was $1.03 \times 10^{5} \pm 0.05 \times 10^{5}$ neutrons cm^{-2} s^{-1} and $5.81 \times 10^{5} \pm 0.41 \times 10^{5}$ photons cm^{-2} s^{-1}, respectively, and the corresponding mass of ^{252}Cf was 54.97 ± 3.88 μg. With respect to neutron dose delivery, the neutron energy spectrum emitted from ^{252}Cf is generally fast and neutrons will typically undergo elastic scatter interactions in blood. Using tabulated energy-dependent microscopic elastic scatter cross-section data for ^{1}H, ^{12}C, ^{16}O and ^{14}N from the ENDF/B-VIII.0 library (*20*), the elastic scatter reaction rate with each element in blood was calculated for each neutron energy bin and the kinetic energy deposited in blood by each such interaction is equal to one half of the sum of the minimum and maximum kinetic energy that can be given to the recoil nucleus in question. Using this approach, the overall absorbed dose rate and absorbed dose delivered to a bare blood volume per unit energy-integrated neutron fluence is calculated to be 10.85 ± 0.54 mGy h^{-1} and 29.25 pGy cm^{2} neutron^{-1}, respectively.

With respect to photon dose delivery, the energy-dependent mass-energy absorption coefficient data for blood (*21*) was utilized to calculate the kerma delivered to a bare blood volume per energy-integrated photon fluence, determined to be 6.32 pGy cm^{2} photon^{-1}. Using the previously stated photon fluence rate incident on the bare blood volume, the kerma rate to the bare blood volume is 13.22 ± 0.93 mGy h^{-1}.

Test tubes were removed from the irradiation facility at pre-determined times, as detailed in Supplementary Table S1 (https://doi.org/10.1667/RR15528.1.S2). A total of five dose points of 12, 30, 60, 90 and 135 mGy were irradiated over two separate days. The lower four dose points were irradiated on the first irradiation day, and the highest dose point was irradiated on the second irradiation day.

Immediately after ^{252}Cf irradiations, whole blood cultures were set up according to IAEA recommendations (*4*). Briefly, 1 ml of whole blood was cultured in 9 ml of Roswell Park Memorial Institute RPMI-1640 medium (Thermo Fisher Scientific™ Inc., Waltham, MA), with 15% fetal bovine serum (Millipore Sigma, Burlington, MA), 100 units ml^{-1} penicillin and 100 μg ml^{-1} streptomycin (Millipore Sigma, Burlington, MA), 20 μ*M* of bromodeoxyuridine (BD Biosciences, San Jose, CA), and 1% phytohemagglutinin (Millipore Sigma). Cultures were incubated in a humidified environment for 48 h at 37°C with 5% carbon dioxide in air. To induce cell cycle arrest in metaphase, 0.1 μg ml^{-1} of colcemid (Thermo Fisher Scientific) was added for the final 4 h of incubation. Cells were further incubated in 0.075 *M* potassium chloride hypotonic solution (Millipore Sigma), followed by three washes with Carnoy's fixative containing three parts methanol to one part acetic acid. Slide making was completed using the Hanabi-HS Metaphase Spreader (Transition Technologies Inc., Toronto, Canada). Fluorescence-plus-Giemsa staining was completed by immersing slides in 20 μg ml^{-1} bisbenzimide H 33258 (Millipore Sigma), then layered with 0.6 *M* sodium phosphate (pH 9.0) (Millipore Sigma) and exposed to a 365 nm ultraviolet light. Slides were washed three times in ultra-pure water, and stained for 10 min in 10% Giemsa Stain (Thermo Fisher Scientific) in Gurr buffer (Thermo Fisher Scientific Inc.). Cover slips were mounted using permount mounting media (Thermo Fisher Scientific).

Slides were coded and metaphase spreads were imaged using the CytoVision® microscope system (Leica Biosystems, Buffalo Grove, IL). Complete metaphase spreads were scored manually according to the dicentric chromosome assay (DCA) criteria laid out in the IAEA Cytogenetic Dosimetry publication (*4*). Briefly, centromeres were counted to ensure metaphase spread completeness. If 46 centromeres were found, metaphase spreads were then examined for the presence of dicentric chromosomes, centric ring chromosomes and acentric fragments. Both dicentric and centric ring chromosomes were included in the aberrations tally, while acentric rings, minutes and terminal deletions were recorded as acentric fragments, following the IAEA Cytogenetic Dosimetry guidelines (*4*).

Data analysis was also carried out as recommended by the IAEA (*4*). The results of the DCA were tested for compliance with the Poisson distribution by calculating the dispersion index and *u*-test statistic for all doses. The goodness of fit of the dose-response curves was evaluated using the Chi-square test (χ^2), and the significance of the equation coefficients was evaluated using the *z* test. *P* values less than 0.05 were considered statistically significant. The Dose Estimate software package (version 5.2) was used to ensure proper curve fitting (*22*). Errors were reported as either standard deviation (SD), the square root of the number of observations or as standard error (SE).

RESULTS

The PHITS simulations revealed that the neutron absorbed dose rate, delivered to a bare blood volume and to a blood volume inside a tube holder, was 10.49 ± 0.52 mGy h^{-1} for both conditions. This dose rate is of the same order of magnitude (difference = 21%) as the ambient dose equivalent rate (8.47 ± 0.42 mGy h^{-1}) obtained from the product of the average ambient dose equivalent per unit fluence for the ^{252}Cf neutron energy spectrum, 385 pSv cm^{2} neutron^{-1} (*23*), and the neutron fluence rate incident on the blood volume, 1.03 × 105 ± 5.13 × 103 neutrons cm^{-2} s^{-1}, divided by the spectrum-averaged w_R value for ^{252}Cf of 16.85. As discussed in (*3*), the ambient dose equivalent per unit fluence was estimated from the dose equivalent per unit fluence delivered by an expanded and aligned planar neutron source to a point located 10 mm into the interior of a 30-cm diameter International Commission on Radiation Units and Measurements tissue sphere. Therefore, the absorbed dose rate delivered to the blood volume in tube and the ambient dose equivalent rate being of the same magnitude indicates that for the ^{252}Cf neutron energy spectrum, dose delivery to blood is an adequate representative of dose delivery to deep organs.

TABLE 2
^{252}Cf-Induced Chromosome Aberration Distribution in Human Peripheral Blood Lymphocytes

Total dose (mGy)	[n] Dose (mGy)	[γ] Dose (mGy)	Cells scored	Total aberr. (±SD)	Distribution of aberrations 0	1	2	3	Total aberr. per cell	[n] Aberr. per cell	[γ] Aberr. per cell	Disp. index (σ^2/y)	*u* Value	RBE [n + γ]	RBE[n]
0	0	0	1,100	1 ± 1	1,099	1	0	0	0.001	0.001	0.000	1.00	-	-	-
12	7	5	1,000	11 ± 3	989	11	0	0	0.011	0.011	0.000	0.99	–0.23	12	20
30	17	13	1,000	37 ± 6	967	29	4	0	0.037	0.036	0.001	1.18	**4.09**	13	23
60	34	26	1,000	63 ± 8	942	53	5	0	0.063	0.061	0.002	1.10	**2.18**	10	17
90	51	39	1,000	77 ± 9	929	66	4	1	0.077	0.074	0.003	1.11	**2.38**	8	13
135	76	59	1,000	159 ± 13	859	124	16	1	0.159	0.155	0.004	1.08	**1.82**	8	15

Notes. Non-Poisson over-dispersed distributions with *u* values approaching or greater than 1.96 are shown in bold face. Aberr. = aberrations; Disp. = dispersion.

The photon absorbed dose rates, delivered to a bare blood volume and to a blood volume inside the tube holder, are 7.54 ± 0.53 mGy h^{-1} and 8.09 ± 0.57 mGy h^{-1}, respectively. The increase in the absorbed dose rate in the presence of the tube holder is attributed to secondary electrons created in the tube wall, from incident photon interactions, being able to enter the blood volume and depositing their kinetic energy. The total absorbed dose rate delivered to the blood volume in the tube holder from incident neutrons and incident photons is 18.58 ± 0.77 mGy h^{-1}.

A total of 6,100 cells were examined across six dose points bearing, in total, 348 dicentric and centric ring chromosome aberrations (Table 2). As a function of dose, the ^{252}Cf aberration yield varied from 1 aberration in 1,100 metaphase spreads at 0 mGy, to 159 aberrations in 1,000 spreads at 135 mGy. Therefore, the background yield was 0.001 aberrations per cell, and the maximum aberration yield was 0.159 aberrations per cell. The majority of cells had no aberrations, with a small portion of cells exhibiting between one and three dicentric and/or centric ring chromosomes. Figure 2 illustrates the ^{252}Cf dose-response relationship compared to the extrapolated ^{137}Cs reference radiation dose-response curve. The quality of the data was tested by calculating the dispersion index (σ^2/y) and the *u*-test statistic. The dispersion index was assessed by dividing the variance by the mean, where a dispersion index of unity

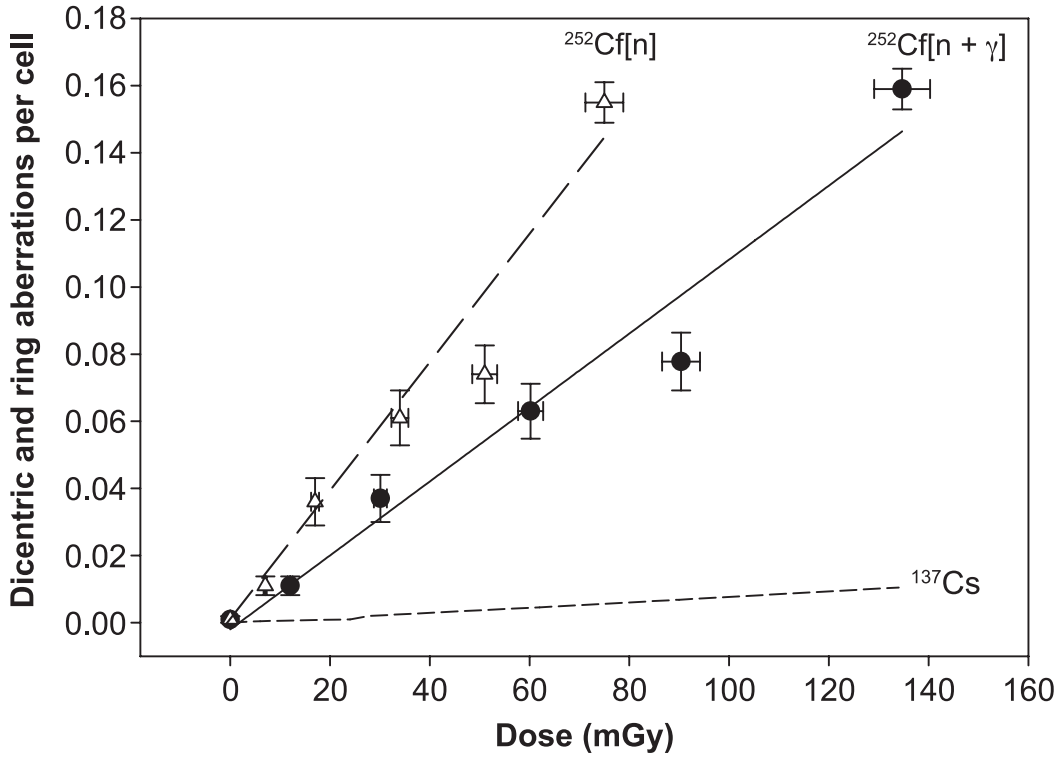

FIG. 2. ^{252}Cf[n + γ] (filled circles, solid line) and ^{252}Cf[n] (open triangles, long-dashed line) linear dose-response regression compared to the extrapolated ^{137}Cs (short-dashed line) dose-response curve (*13*) detailing the relationship between radiation dose and the number of dicentric and centric ring chromosome aberrations per cell. Error bars represent standard error of the mean.

TABLE 3
^{252}Cf Neutron and ^{137}Cs Photon-Induced DCA Linear (L) and Linear-Quadratic (LQ) Dose-Response Regression and R^2 Values

Radiation	Regression	α [±SE] (Gy^{-1})	β [±SE] (Gy^{-2})	c [±SE]	R^2
^{252}Cf[n + γ]	L: $A = 0.0008 + 1.0490D$	1.0490 ± 0.0747	-	0.0008 ± 0.0042	0.96
	LQ: $A = 0.0010 + 0.9238D + 1.2950D^2$	0.9238 ± 0.2112	1.2950 ± 2.0500	0.0010 ± 0.0013	0.97
^{252}Cf[n]	L: $A = 0.0008 + 1.7990D$	1.7990 ± 0.1355	-	0.0008 ± 0.0057	0.96
	LQ: $A = 0.0009 + 1.5610D + 4.3650D^2$	1.5610 ± 0.3807	4.3650 ± 6.5670	0.0009 ± 0.0013	0.97
^{137}Cs[γ] (*13*)	$A = 0.070D + 0.061D^2$	0.070 ± 0.0088	0.061 ± 0.0043	-	n/a

Note. A = aberrations per cell; α, β, c = regression coefficients; D = dose (Gy); R^2 = coefficient of determination.

indicates alignment with the Poisson distribution. Results above 1.96 indicated a non-Poisson over-dispersion at the 5% significance level (*4, 24*). Three of the five exposure data points, i.e., 30 mGy, 60 mGy and 90 mGy, demonstrated elevated dispersion and u values >1.96 indicating non-Poisson over-dispersion (Table 2). The 135 mGy dose point was nearing a significant over-dispersion, with a u value of 1.82.

The linear and linear-quadratic dose-response relationships for ^{252}Cf dicentric and centric ring aberrations (A) were calculated using the iteratively reweighted least-squares method recommended by the IAEA for both the neutron plus photon [n + γ] and neutron [n] dose components (*4, 22*). The neutron-only aberrations were calculated using the method proposed by Lloyd *et al.* (*7*) by extrapolating the number of photon-induced aberrations per cell at each dose point based on the previously published in-house ^{137}Cs dose-response curve (*13*). This value was then subtracted from the total aberrations per cell to give the neutron aberrations per cell (Table 1). Linear and linear-quadratic regression equations and their errors are given in Table 3. Where χ^2 was greater than the degrees of freedom (df), the standard error was increased by $(\chi^2/df)^{1/2}$. All fits demonstrated non-significant χ^2-test P values (Table 4) that indicated the observed data points did not differ from the fitted data, confirming a good dose-response curve fit. The z test indicated the β coefficient was not significant for both linear-quadratic fits, confirming a preference for a linear dose-response curve for both the [n + γ] and [n] data (Table 4).

RBE_M was calculated as a ratio of the ^{252}Cf and the ^{137}Cs photon α coefficient values that represent the linear component of the dose-response curves, as shown in Table 3. A previously published ^{137}Cs linear-quadratic dose response for aberrations from an earlier CNL study was used as the photon reference exposure (Table 3) (*13*). Consequently, a linear dose-response relationship for the neutron and photon components of ^{252}Cf revealed a RBE_M[n + γ] of 15.0 ± 2.6 and a RBE_M[n] of 25.7 ± 3.8 for dicentric plus centric ring induction.

Dose-specific RBE values for the five ^{252}Cf exposures were also calculated by dividing the ^{137}Cs photon dose required to generate a given effect by the ^{252}Cf dose that gave the same effect, as evaluated in Table 2.

TABLE 4
***P* Values for *z* Test and Chi-Square Test of Linear (L) and Linear-Quadratic (LQ) Dose-Response Curve Fitting**

	z Test significance		Chi-square test significance
	α	β	χ^2
^{252}Cf[n + γ] L	0.0001	-	0.5806
^{252}Cf[n + γ] LQ	0.0221	0.5725	0.1210
^{252}Cf[n] L	0.0002	-	0.5653
^{252}Cf[n] LQ	0.0262	0.5538	0.1011

DISCUSSION

In the current study, we analyzed and report here on the DNA aberration dispersion, which, to our knowledge, had not previously been reported for high-LET ^{252}Cf exposure of ~2.1 MeV neutrons. Dicentric chromosomes and (much rarer) ring chromosomes were both included in the analysis (*4*). Four of five dose points were found to exhibit, or were close to exhibiting, non-Poisson over-dispersion (Table 2). The statistical power is low at the lowest dose. Only the lowest exposure dose point of 12 mGy, with the higher uncertainty of 11 ± 3 aberrations in 1,000 cells, did not approach or achieve over-dispersion. It is possible that increasing the number of cells scored could eventually result in the predicted high-LET over-dispersion at all dose points. However, due to the limited sample available for this study, it was not possible to explore this option. Non-Poisson over-dispersion is characteristic of high ionization density and has been observed in other neutron studies, including those at similar fast neutron energies of 1.151 MeV (*6*), 1.6 MeV (*25*) and 4.85 MeV (*6*).

Linear and linear-quadratic regression fits were both evaluated, revealing a stronger relationship for the linear dose-response function due to the non-significant linear-quadratic β coefficient (Table 4). Both previously published ^{252}Cf studies report linear dose-response relationships (*7, 8*). Other DCA studies in human lymphocytes with neutron energies between thermal and 1.151 MeV predominantly report linear dose-response relationships (*6, 14, 26–28*), while higher energies tend to show a mix of linear and linear-quadratic fits (*6–8, 25, 26, 29–32*).

There are currently two other published studies detailing ^{252}Cf RBE for human lymphocytes. Lloyd *et al.* (*7*) described RBE [n] values ranging from 6 to 27 for ^{252}Cf neutron doses

between 118–2,894 mGy, in reference to ^{60}Co photons at a similar dose rate (Table 1). Tanaka *et al.* (*8*) investigated several dose rates and found that dose-specific ^{252}Cf RBE ranged from 2.3 to 7.7 for dicentric aberration yields at 1,000 mGy when ^{252}Cf neutron and photon doses were considered together, and 3.3–12.0 when the neutron component of the dose was considered alone. These values were generated in reference to either ^{60}Co or ^{137}Cs photons at matched dose rates. For easier comparison here, the RBE_M values for both prior studies were calculated using their data. For the study by Lloyd *et al.* (*7*), the $RBE_M[n + \gamma]$ was found to be 24 ± 11 and the $RBE_M[n]$ was of 33 ± 15. For Tanaka *et al.* (*8*), $RBE_M[n + \gamma]$ values ranged from 6.3 to 7.7, and the $RBE_M[n]$ values were between 9.8 to 11.9, with lower-dose-rate exposures generating a slightly higher RBE_M (Table 1). In both cases, the DCA data conformed to a linear dose relationship, and the calculated RBE_M values were similar to the highest reported dose-specific RBE.

For the current study, a $RBE_M[n + \gamma]$ of 15.0 ± 2.6 was evaluated for the combined neutron and photon components of ^{252}Cf, and an $RBE_M[n]$ of 25.7 ± 3.8 was found for only the neutron component of ^{252}Cf, compared to ^{137}Cs photons. This was based on a thorough examination of 1,000–1,100 metaphase spreads per dose point (Table 2). Both the $RBE_M[n + \gamma]$ and $RBE_M[n]$ values fall between RBE_M values of Lloyd *et al.* (*7*) ($RBE_M[n + \gamma] = 24 \pm 11$, $RBE_M[n] = 33 \pm 15$) and Tanaka *et al.* (*8*) ($RBE_M[n + \gamma] = 6.3 - 7.7$, $RBE_M[n] = 9.8 - 11.9$). The $RBE_M[n]$ reported here (25.7) is similar to the RBE_M reported for other fast neutron energies, including 4.85 MeV mono-energetic neutrons (RBE_M of 32.3 ± 13.3) (*6*), and is higher than the ICRP w_R value of 16.85 for ^{252}Cf neutrons (*9, 10*).

The ^{137}Cs reference photon curve was generated using much higher absorbed doses (500 mGy to 3,500 mGy) than in the current ^{252}Cf study (*13*). Thus, it was necessary to extrapolate the photon data, given that it is not practical to score photon DNA aberrations that are statistically viable at the very low absorbed dose range reported here. Most of the neutron RBE_M values reported in the literature, including those of Lloyd *et al.* (*7*), are derived using ^{60}Co as the reference radiation source (*6, 14, 26–30, 32*). RBE_M can be affected by the reference radiation source, and using ^{60}Co as a reference radiation can result in a higher, but not statistically different, RBE_M compared to ^{137}Cs (*26*).

Dose-specific $RBE[n + \gamma]$ decreased from 12 and 13 to 8 with increasing doses ranging from 12 mGy and 30 mGy to 135 mGy (Table 2). The dose-specific RBE[n] also demonstrated an overall decrease with increasing dose, with the highest RBE of 23 at 7 mGy and the lowest RBE of 13 found at 51 mGy (Table 2). This trend is consistent with previously reported studies (*7, 8*). As expected, the highest dose-specific $RBE[n + \gamma]$ and RBE[n] values of 13 and 23 are similar to the RBE_M of 15.0 ± 2.6 and 25.7 ± 3.8 reported previously.

There was a dose-rate discrepancy between the ^{252}Cf irradiations reported here (18.58 ± 0.77 mGy h^{-1}) and the ^{137}Cs reference radiation (49,800 mGy h^{-1}). Given the very low dose rate of the ^{252}Cf source, a matched dose and dose-rate reference radiation curve was not practical. Instead, a previously published higher-dose-rate ^{137}Cs dose-response curve was used for the reference radiation. Dose-rate discrepancies between neutron and reference radiations have been noted in several other DCA RBE studies (*27, 28*). Lloyd *et al.* (*7*) and Tanaka *et al.* (*8*) used matched or nearly-matched ^{252}Cf and reference radiation dose rates. However, the dose rates used by Tanaka *et al.* (*8*) were 1,200 mGy h^{-1}, 120 mGy h^{-1} or 12 mGy h^{-1}, and the highest RBE of 7.7 was reported after γ-ray and neutron irradiations at the lowest dose rate of 12 mGy h^{-1}. Similar $RBE[n + \gamma]$ values of 7.6 and 7.7 were reported by Tanaka *et al.* (*8*) for dose rates of 120 mGy h^{-1} and 12 mGy h^{-1}, respectively, the lower value being of the same order as the dose rate of 18.58 mGy h^{-1} used here. It is already well-established that low-LET radiation effects are susceptible to dose-rate variations and long irradiation times (*4*), and the 12 mGy h^{-1} ^{137}Cs reference radiation curve used by Tanaka *et al.* (*8*) included protracted photon irradiation times. It is possible this would have drastically affected the scope of chromosome aberrations available for assessment, resulting in an elevated RBE.

CONCLUSION

To our knowledge, this work represents the first measurements for a dicentric and ring chromosome dose response after low-dose ^{252}Cf$[n + \gamma]$ exposures (12–135 mGy), and for DNA aberration distribution data after dicentric chromosome analysis of ^{252}Cf-irradiated whole blood. A linear dose-response relationship was found for peripheral blood lymphocytes with $RBE_M[n + \gamma]$ and $RBE_M[n]$ values of 15.0 ± 2.6 and 25.7 ± 3.8, respectively. Future work should allow for better dose-rate matching of neutron and photon dose response, and more robust scoring of the aberrations in the low-dose range to further evaluate DNA aberration dispersion at all dose points.

SUPPLEMENTARY INFORMATION

Table S1. Detailed ^{252}Cf neutron irradiation plan.

ACKNOWLEDGMENTS

This work was funded through Atomic Energy of Canada Limited's Federal Science and Technology Program. We gratefully acknowledge the CNL Health Centre staff for performing routine phlebotomy in support of this research project.

Received: September 24, 2019; accepted: October 30, 2020; published online: December 30, 2020

REFERENCES

1. Martin RC, Knauer JB, Balo PA. Production, distribution and applications of californium-252 neutron sources. Appl Radiat Isot 2000; 53:785–92.
2. Martin RC, Glasgow DC, Martin MZ. Applications of californium-

252 neutron irradiations and other nondestructive examination methods at Oak Ridge National Laboratory. In: Laue CA, Nask KL, editors. Radioanalytical methods in interdisciplinary research. Washington: American Chemical Society; 2003. p. 88–104.

3. Ali F, Atanackovic J, Boyer C, Festarini A, Kildea J, Paterson LC, et al. Dosimetric and microdosimetric analyses for blood exposed to reactor-derived thermal neutrons. J Radiol Prot 2018; 38:1037–52.
4. Cytogenetic dosimetry: applications in preparedness for and response to radiation emergencies. Vienna, Austria: International Atomic Energy Agency; 2011.
5. Relative biological effectiveness (RBE), quality factor (Q), and radiation weighting factor (WR). ICRP Publication 92. Ann ICRP 2003; 33:1–117.
6. Schmid E, Schlegel D, Guldbakke S, Kapsch RP, Regulla D. RBE of nearly monoenergetic neutrons at energies of 36 keV–14.6 MeV for induction of dicentrics in human lymphocytes. Radiat Environ Biophys 2003; 42:87–94.
7. Lloyd DC, Purrott RJ, Reeder EJ, Edwards AA, Dolphin GW. Chromosome aberrations induced in human lymphocytes by radiation from 252Cf. Int J Radiat Biol Relat Stud Phys Chem Med 1978; 34:177–86.
8. Tanaka K, Gajendiran N, Kamada N. Relative biological effectiveness (RBE) and dose rate dependent ratio of translocation to dicentric chromosome yield in 252Cf neutrons. Indian J Sci Technol 2009; 2:1–11.
9. International Commission on Radiological Protection. The 2007 recommendations of the International Commission on Radiological Protection. ICRP Publication 103. Ann ICRP 2007; 37:1–332.
10. Hall EJ, Rossi HH. Californium-252 in teaching and research. Vienna, Austria: International Atomic Energy Agency; 1974.
11. Virsik RP, Harder D. Statistical interpretation of the overdispersed distribution of radiation-induced dicentric chromosome aberrations at high LET. Radiat Res 1981; 85:13–23.
12. Flegal FN, Devantier Y, McNamee JP, Wilkins RC. QuickScan dicentric chromosome analysis for radiation biodosimetry. Health Phys 2012; 98:276–81.
13. Flegal FN, Devantier Y, Marro L, Wilkins RC. Validation of Quickscan dicentric chromosome analysis for high throughput radiation biological dosimetry. Health Phys 2012; 102:143–53.
14. Schmid E, Wagner FM, Canella L, Romm H, Schmid TE. RBE of thermal neutrons for induction of chromosome aberrations in human lymphocytes. Radiat Environ Biophys 2013; 52:113–21.
15. Neutron Survey Meter, Model REM 500. Goleta, CA: Far West Technology, Inc. (https://bit.ly/2TRyjvT)
16. Sato T, Iwamoto Y, Hashimoto S, Ogawa T, Furuta T, Abe S, et al. Features of Particle and Heavy Ion Transport code System (PHITS) current version 3.02. J Nucl Sci Technol 2018; 55:684–90.
17. McConn Jr. RJ, Gesh CJ, Pagh RT, Rucker RA, Williams III RG. Compendium of material composition data for radiation transport modeling revision 1 (PIET-43741-TM-963, PNNL-15870 Rev. 1). Richland, WA: Pacific Northwest National Laboratory; 2011.
18. Reference neutron radiations Part 1: Characteristics and methods of production. ISO 8529-1). Geneva, Switzerland: International Organization for Standardization; 2000.
19. Atanackovic J, Yonkeu A, Dubeau J, Witharana SH, Priest N. Characterization of neutron fields from bare and heavy water moderated 252Cf spontaneous fission source using Bonner sphere spectrometer. Appl Radiat Isot 2015; 99:122–32.
20. Evaluated Nuclear Data File (ENDF). Vienna, Austria: International Atomic Energy Agency; c2018. (https://bit.ly/3kK4AAz)
21. Blood, whole (ICRU-44). Gaithersburg, MD: National Institute of Standards and Technology. (https://bit.ly/3oJ8KLl)
22. Ainsbury EA, Lloyd DC. Dose estimation software for radiation biodosimetry. Health Phys 2010; 98:290–5.
23. Reference neutron radiations Part 3: Calibration of area and personal dosimeters and determination of their response as a function of neutron energy and angle of incidence. ISO 8529-3. Geneva, Switzerland: International Organization for Standardization; 2001.
24. Szluinska M, Edwards AA, Lloyd DC. Statistical methods for biological dosimetry. In: Obe G, Vijayalaxmi, editors. Chromosomal alterations. Berlin/Heidelberg: Springer; 2007. p. 351–70.
25. Schmid E, Schraube H, Bauchinger M. Chromosome aberration frequencies in human lymphocytes irradiated in a phantom by a mixed beam of fission neutrons and gamma-rays. Int J Radiat Biol 1998; 73:263–7.
26. Lloyd DC, Purrott RJ, Dolphin GW, Edwards AA. Chromosome aberrations induced in human lymphocytes by neutron irradiation. Int J Radiat Biol Relat Stud Phys Chem Med 1976; 29:169–82.
27. Schmid E, Regulla D, Guldbakke S, Schlegel D, Bauchinger M. The effectiveness of monoenergetic neutrons at 565 keV in producing dicentric chromosomes in human lymphocytes at low doses. Radiat Res 2000; 154:307–12.
28. Schmid E, Regulla D, Guldbakke S, Schlegel D, Roos M. Relative biological effectiveness of 144 keV neutrons in producing dicentric chromosomes in human lymphocytes compared with 60Co gamma rays under head-to-head conditions. Radiat Res 2002; 157:453–60.
29. Bauchinger M, Koester L, Schmid E, Dresp J, Streng S. Chromosome aberrations in human lymphocytes induced by fission neutrons. Int J Radiat Biol Relat Stud Phys Chem Med 1984; 45:449–57.
30. Fabry L, Leonard A, Wambersie A. Induction of chromosome aberrations in G0 human lymphocytes by low doses of ionizing radiations of different quality. Radiat Res 1985; 103:122–34.
31. Bauchinger M, Schmid E, Rimpl G, Kuhn H. Chromosome aberrations in human lymphocytes after irradiation with 15.0-MeV neutrons in vitro. I. Dose-response relation and RBE. Mutat Res 1975; 27:103–9.
32. Nolte R, Muhlbradt KH, Meulders JP, Stephan G, Haney M, Schmid E. RBE of quasi-monoenergetic 60 MeV neutron radiation for induction of dicentric chromosomes in human lymphocytes. Radiat Environ Biophys 2005; 44:201–9.